Gold Nanowires and Their Chemical Modifications

Hannu Häkkinen, Robert N. Barnett, and Uzi Landman*

School of Physics, Georgia Institute of Technology, Atlanta, Georgia 30332-0430

Received: August 5, 1999; In Final Form: September 1, 1999

Equilibrium structure, local densities of states, and electronic transport in a gold nanowire made of a four-atom chain supported by two gold electrodes, which has been imaged recently by high-resolution electron microscopy, and chemical modification of the wire via the adsorption of a methylthiol molecule, are investigated with ab initio local density functional simulations. In the bare wire at the imaged geometry the middle two atoms dimerize, and the structure is strongly modified by the adsorption of the molecule with an accompanying increase of the ballistic conductance through the wire.

Generation of wires of atomic scale dimensions in the process of formation and/or elongation of interfacial contacts has been predicted through early molecular dynamics simulations using many-body potentials,[1,2] and in the face of fundamental interest and technological considerations driven by the relentless miniaturization of electronic and mechanical devices such wires have been the subject of intensive experimental and theoretical research endeavors.[3] Indeed, nanometer-scale wires (nanowires, NWs) have been created, and their structural, mechanical, and transport characteristics were studied using a variety of techniques,[3] including most recently combined scanning tunneling microscopy (STM) and direct imaging with the use of high-resolution transmission electron microscopy.[4−6]

We report here on ab initio local-density functional (LDA) investigations[7] of the atomic structure, electronic spectrum, and conductance of a gold NW consisting of a four-atom chain connected to gold electrodes, which is the smallest NW imaged by HRTEM.[6,8] Our study reveals dimerization of the gold atoms in the middle of the chain[8] akin to a Peierls transition in (extended) one-dimensional systems. Furthermore, we explore structural and electronic spectral modifications resulting from adsorption of a molecule (methylthiol, SCH_3) to the wire,[9] demonstrating the sensitivity of these properties to such chemical interactions, as well as their effect on the electronic conductance of the wire which we find to increase upon adsorption. These results provide a new interpretation of the measured HRTEM image of the atomic gold wire[6,8] and suggest a new strategy for formation of organo-metallic NWs, as well as the use of NWs as monitoring and chemical sensing devices.

In light of the aforementioned STM/HRTEM observations,[6,8] we start our simulation from a four-atom Au wire consisting of two tip-atoms (t) located at the apexes of two opposing tip-electrodes distanced initially by $d_{tt}(0) = 8.9$ Å, and of two internal Au atoms (i) located in the gap between the two electrodes with initial uniform distances $d_{ti}(0) = d_{ii}(0) = 2.967$ Å between neighboring atoms of the wire; the tip-electrodes consist each of 29 gold atoms arranged in a pyramidal shape made of face-centered-cubic stacked (110) layers and exposing (100) and (111) facets, with the tip atoms (as well as the internal wire atoms) and the atoms of the underlying layers supporting them treated dynamically, while the rest of the electrode gold atoms are held at their crystalline lattice positions. This initial structure relaxes spontaneously in the course of a total energy minimization with a 0.16 eV gain in the total energy, to that shown in Figure 1 (AuNW, left) where the two inner-wire atoms dimerize, with $d_{ii} = 2.68$ Å (compared to d (Au−Au) = 2.48 Å in a free Au_2 molecule), $d_{ti} = 3.07$ Å, and the total length of the wire shortens to $d_{tt} = 8.82$ Å.[10]

From the local density of states (LDOS) of the dimerized wire (Figure 2), calculated in the regions delineated in Figure 1 (AuNW, left), we observe that the electronic states in the interior region of the wire (region E, see Figure 1, left) near the Fermi energy (E_F, marked by a dashed line in Figure 2) are not found in the free Au_2 dimer (whose states are marked by dots on the upper energy axis of Figure 2). Rather, these states originate from hybridization between the atomic states of the interior Au atoms and the gold-electrode states, with the highest-occupied molecular orbital (HOMO) exhibiting a dominant d-character on the interior wire atoms. The dimerization is driven by lowering of the energies of states in the interval $-10 \le E \le -6.5$ eV calculated at the interior region of the wire (compare the upper and lower LDOS curves in the inset to Figure 2, corresponding to the dimerized and initial equal-distance configurations, respectively). Additionally, the dimerization of the wire is accompanied by a small increase of the energy gap near E_F from 0.194 eV in the equidistant wire to 0.216 eV in the dimerized one; in a certain sense the observed dimerization may be regarded as a "predecessor" of a Peierls transition, though such description should be treated with caution due to the rather limited extent of the wire considered here. The calculated electronic conductance[11] of the dimerized AuNW is $G = 0.58 g_0$ ($g_0 = 2e^2/h$, where e is the electron charge and h is the Planck constant) corresponding to a resistance of 22.17 kΩ, and ballistic transport occurs through a single conductance channel.[11]

Two binding configurations of a methylthiol molecule to the dimerized equilibrium configuration of the AuNW were considered: (i) the SCH_3 molecule bonded to the two middle interior Au atoms of the wire (see AuNW/m-SCH_3 in Figure 1), and (ii) binding of the molecule to a terminal tip atom (t) of the wire and to the neighboring interior wire atom (see AuNW/t-SCH_3 in Figure 1). The binding energies of the molecule in the two adsorption configurations are essentially the same (4.01 eV), and in both cases binding of the molecule is accompanied by significant structural changes of the wire. In the m-SCH_3

* Corresponding author.

10.1021/jp992787p CCC: $18.00
Published on Web 09/25/1999

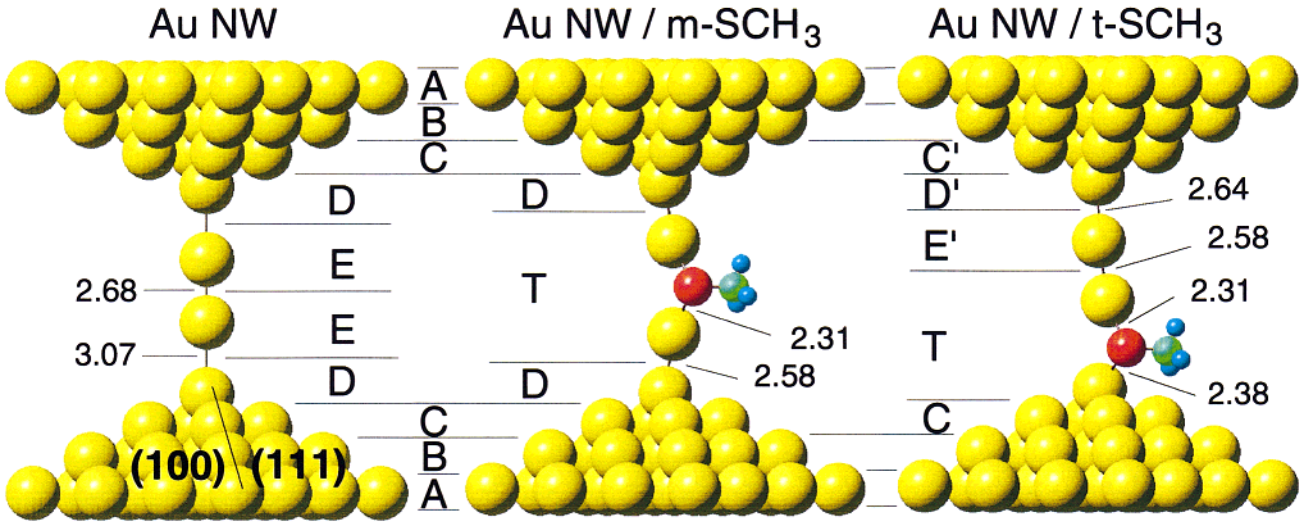

Figure 1. Equilibrium structures of a bare gold nanowire (AuNW, left) and of wires chemically modified by adsorption of a SCH_3 molecule, with the molecule adsorbed in the middle of the wire (m-SCH_3) or at the vicinity of the tip (t-SCH_3). The bare four-atom wire consists of two tip atoms (t) and two interior atoms (i), and it is supported by two opposing fcc gold electrodes exposing (100) and (111) facets, with the wire axis along the [110] direction. Yellow spheres correspond to Au atoms, and in the chemically modified wires S, C, and H atoms are depicted by red, green, and blue spheres, respectively. The length of the dimerized bare AuNW $d_{tt} = 8.82$ Å, and those of the AuNW/m-SCH_3 and AuNW/t-SCH_3 wires are 9.02 and 8.98 Å, respectively. Regions in the wires used for LDOS calculations (see Figures 2 and 3) are denoted by letters. Marked distances are in units of Å.

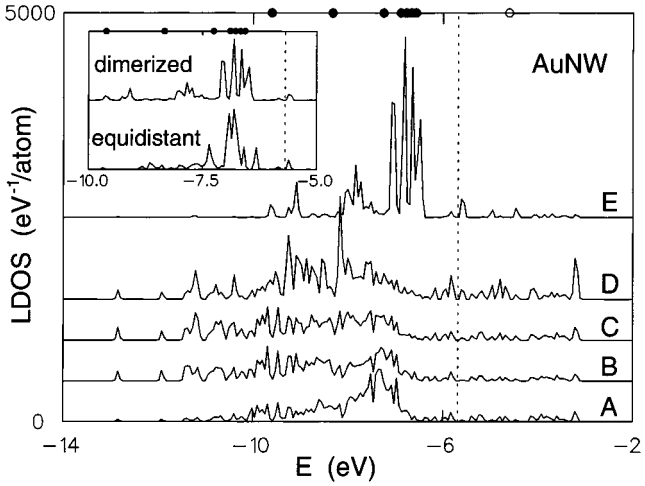

Figure 2. Local densities of states (LDOS) for the dimerized AuNW. Different curves are marked by letters corresponding to the regions delineated in Figure 1 (left), and they are vertically shifted with respect to each other for clarity. Displayed in the inset are the LDOS calculated in the interior region (E) of the dimerized wire (upper curve) and the initial equidistant wire (lower curve). The Fermi energy ($E_F = -5.68$ eV) is denoted by a dashed line. The molecular eigenvalues of a free gold dimer (Au_2) are marked by dots on the upper axis (filled and empty dots correspond to occupied and unoccupied states, respectively). Energy in units of eV and LDOS in eV^{-1} /atom.

configuration (Figure 1, middle) the dimerization of the interior wire gold atoms is removed, and the sulfur atom is bonded to the two interior gold atoms with d (S−Au) = 2.31 Å, the angle ∠ (Au−S−Au) = 117.4°, and d (S−C) = 1.84 Å. The configuration is symmetric about a plane of reflection passing through the sulfur atom normal to the plane of the figure, and the length of the wire increases by 0.1 Å (i.e., $d_{tt} = 9.02$ Å), with $d_{ti} = 2.58$ Å and $d_{ii} = 3.94$ Å; the wire atoms are shifted slightly in the direction of the adsorbed molecule with the terminal wire atoms displaced laterally by 0.016 Å from the 4-fold hollow site of the underlying gold electrode layer. Dimerization of the interior gold wire atoms is removed also in the t-SCH_3 equilibrium bonding configuration where symmetry is broken, the bond lengths of the sulfur to the two gold atoms are unequal [d (S−Au(t)) = 2.38 Å and d (S−Au(i)) = 2.31 Å], the angle ∠ (Au(t)−S−Au(i)) = 109.3°, $d_{ti} = 3.83$ Å, d (S−C) = 1.85 Å, and the length of the wire is $d_{tt} = 8.98$ Å; additionally, the Au(t) atom bonded to the sulfur is displaced laterally by 0.057 Å from the 4-fold hollow site, while the displacement of the other Au(t) atom (not bonded directly to the molecule) is 0.012 Å. We remark that in both adsorption configurations the intra-thiol d (S−C) distance, as well as the S−Au bond length are similar to those calculated for the equilibrium structure of a free Au_2 SCH_3 molecule where d (S−C) = 1.84 Å and d (S−Au) = 2.41 Å, while the Au−S−Au angles in the thiolated wires are much larger than in the free molecule (where ∠ (Au−S−Au) = 67.1°) due to the binding of the sulfur-bonded gold atoms of the wire to the rest of the nanostructure.

Examination of the LDOS for the chemically modified wires displayed in Figure 3 reveals that changes from the spectrum of the bare dimerized wire (Figure 2) are localized to regions in the immediate vicinity of the molecular binding site (compare region E in Figure 2 with region T for AuNW/m-SCH_3 and regions T and E′ for AuNW/t-SCH_3 in Figure 3). In both cases E_F lies below the HOMO level of the free SCH_3 molecule correlating with energy gain due to hybridization of the molecular states with the states of the wire. In both of the chemically modified wires the HOMO level is partially occupied (containing about one hole) while it is doubly occupied in the bare AuNW, and the gap between that level and the lowest unoccupied one is 0.21 and 0.316 eV in the m-SCH_3 and t-SCH_3, respectively.

Chemical modifications of the AuNW are signaled, and may be detected, by changes in the electronic conductance, which increases upon adsorption, i.e., G (AuNW/m-SCH_3) = $0.82g_0$ and G (AuNW/t-SCH_3) = $0.88g_0$, involving a single conductance channel. While at first sight an increase of the conductance in the presence of an adsorbate may seem surprising, it can be explained via examination of the potential landscapes governing the propagation of the electron through the wires (see Figure 4). Comparison between the potential shown in Figure 4a for the bare dimerized nanowire with those corresponding to the

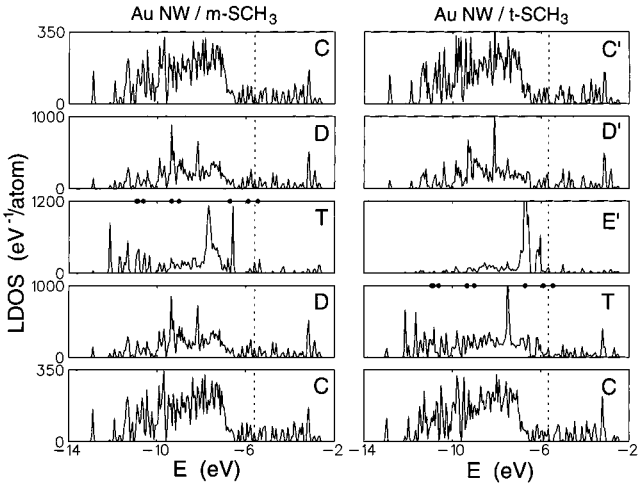

Figure 3. LDOS for chemically modified AuNW, with a SCH_3 molecule adsorbed at the middle of the wire (AuNW/m-SCH_3, left) and at the tip-vicinity (AuNW/t-SCH_3, right). Different curves marked by letters correspond to regions delineated in Figure 1. In regions T, which include the adsorbed thiol molecule, occupied states of the free SCH_3 molecule are denoted by filled dots on the upper axis. The Fermi energy is denoted by a dashed line; $E_F = -5.59$ eV and -5.66 eV for the m-SCH_3 and t-SCH_3 adsorption configurations. Energy in units of eV and LDOS in eV^{-1} /atom.

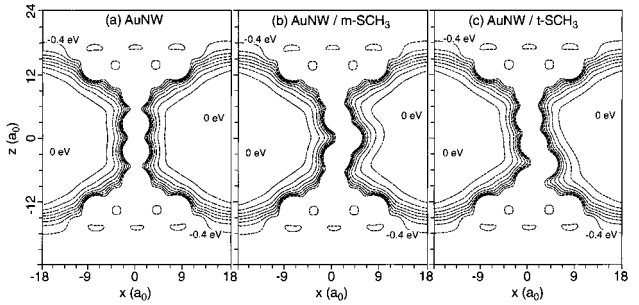

Figure 4. Potential profiles [11] in cross-sectional cuts through the bare AuNW dimerized wire (a) and through the chemically modified ones (b and c). The vacuum level is at zero and the potential step between adjacent contours is 0.05 eV. Note the potential bottlenecks for the bare dimerized wire (a), which are highly reduced in the chemically modified nanowires. Energy in units of eV and distances in Bohr radius (a_0).

chemically modified ones (Figure 4 parts b and c), reveals that the potential barriers (bottlenecks), associated with the unequal spacings between the gold atoms in the dimerized equilibrium structure and the reduced overlap between the electronic states of the inner wire and the tip atoms, which decrease the transmission of the incident electron through the bare AuNW (Figure 4a), are reduced in the chemically modified wires and the conductance path is broadened, resulting in enhancement of the ballistic transmission through these wires.[12]

These findings, obtained through ab initio simulations, pertaining to the dimerized structure of an atomic gold nanowire and the sensitivity of structural, electronic, and conductance properties of such wires to chemical modifications via molecular adsorption, provide a new interpretation of recent HRTEM measurements,[6,8] demonstrate methods for probing the nature of chemical interactions with such nanostructures, and suggest a strategy for preparation of chemically modified nanowires.

Acknowledgment. We thank A. G. Scherbakov for his assistance in conductance calculations. This research is supported by the U.S. DOE, AFOSR, and the Academy of Finland. Calculations were performed on an IBM SP2 parallel computer at the Georgia Tech Center for Computational Materials Science, and on a Cray T3E at the National Energy Research Scientific Computing Center (NERSC) at Berkeley, CA.

References and Notes

(1) Landman, U.; Luedtke, W. D.; Burnham, N. A.; Colton, R. J. *Science* **1990**, *248*, 454.

(2) Landman, U.; Luedtke, W. D. *J. Vac. Sci. Technol.* **1991**, *B9*, 414.

(3) *Nanowires*; Serena, P. A.; Garcia, N., Eds.; Kluwer: Dordrecht, 1997.

(4) Kizuka, T.; Yamada, K.; Deguchi, S.; Naruse, M.; Tanaka, N. *Phys. Rev. B* **1997**, *55*, R7398.

(5) Kizuka, T. *Phys. Rev. Lett.* **1998**, *81*, 4448.

(6) Ohnishi, H.; Kondo, Y.; Takayanagi, K. *Nature* **1998**, *395*, 780.

(7) The calculations were performed using the ab initio Born−Oppenheimer (BO) local-spin-density (LSD) molecular dynamics method (BO-LSD-MD, for details see Barnett, R. N.; Landman, U. *Phys. Rev. B* **1993**, *48*, 2081) rewritten recently for massively parallel computing. The valence electrons of the Au, S, C, and H atoms (11, 6, 4, and 1 electrons, respectively) are described by norm-conserving nonlocal pseudopotentials (Troullier, N.; Martins, J. L. *Phys. Rev. B* **1991**, *43*, 1993) with a plane-wave basis set (kinetic energy cutoff of 62 Ry). The pseudopotentials core radii (in units of a_0) are as follows (tilde indicates local component): Au: $\tilde{s}(2.50)$, $p(3.00)$, $d(2.00)$; S: $s(1.80)$, $\tilde{p}(2.30)$; C: $s(1.50)$, $\tilde{p}(1.54)$; H: $\tilde{s}(0.95)$. The Au pseudopotential is relativistic and weight-averaged by the degeneracy of $j = l \pm 1/2$ states (Kleinman, L. *Phys. Rev. B* **1980**, *21*, 2630; Bachelet, G. B.; Schluter, M. *Phys. Rev. B* **1982**, *25*, 2103). For a recent study of a $Au_{38}(SCH_3)_{24}$ nanocrystal using the above method, see Häkkinen, H.; Barnett, R. N.; Landman, U. *Phys. Rev. Lett.* **1999**, *82*, 3264, and for an ab initio simulation of sodium nanowires, see Barnett, R. N.; Landman, U. *Nature* **1997**, *387*, 788.

(8) In ref 6 (see Figure 3) an HRTEM image of an 8.9 Å long gold wire was modeled as a four-atom wire with equal spacings between neighboring atoms in the wire. Formation of wires made of gold atom chains has been indirectly inferred also from measurements using mechanically controllable break junction and STM, see Yanson, A. I.; Bollinger, G. Rubio; van der Brom, H. E.; Agraït, N.; van Ruitenbeek, J. M. *Nature* **1998**, *395*, 783.

(9) For an experimental investigation of adsorbate effects on the conductance of gold wires, see Li, C. Z.; Sha, H.; Tao, N. J. *Phys. Rev. B* **1998**, *58*, 6775.

(10) In a similar simulation but starting from a somewhat longer equal-distance wire ($d_{tt}(0) = 9$ Å), the wire also relaxed to a dimerized structure ($d_{ii} = 2.61$ Å, $d_{ti} = 3.29$ Å, and $d_{tt} = 9.19$ Å) with a total energy gain of 0.45 eV. The total energy of the dimerized equilibrium structure of this wire is higher by 0.33 eV than that of the shorter wire discussed in the text.

(11) In calculations of the conductance we used a recursion-transfer-matrix method (see Hirose, K.; Tsukada, M. *Phys. Rev. B* **1995**, *51*, 5278) in conjunction with the LDA self-consistent effective potentials calculated for the geometries shown in Figure 1 and processed according to the procedure described in Nakamura, A.; Brandbyge, M.; Hansen, L. B.; Jacobsen, K. W. *Phys. Rev. Lett.* **1999**, *82*, 1538. In these conductance calculations we used 512 plane-waves to ensure convergence; details of the computations will be published elsewhere. Transformation to nonmixing eigenchannels was performed following Brandbyge, M.; Sorensen, M. R.; Jacobsen, K. W. *Phys. Rev. B* **1997**, *56*, 14956. The total conductance is expressed as $G = g_0 \sum_n |\tau_n|^2$, where $0 \le |\tau_n|^2 \le 1$ is the transmission probability of the nth eigenchannel, and $g_0 = 2e^2/h$. For an experimental procedure of decomposition of the total conductance into a sum of contributions from individual channels, see Scheer, E., et al. *Nature* **1998**, *394*, 154.

(12) We remark that even for the bare gold nanowire the structure and conductance of the nanowire are sensitive to small variations in the spacing between the two electrodes. For example, starting from the equilibrium dimerized structure shown in Figure 1 (left) and reducing the distance between the two opposing electrodes by 0.5 Å (that is, decreasing the distance between the two outermost, static, gold layers), the newly relaxed structure shows a weakening of the dimerization effect of the inner gold atoms (i.e., $d_{ti} = 2.79$ Å, $d_{ii} = 2.71$ Å, and $d_{tt} = 8.29$ Å, compared to the values shown in Figure 1 (left)), the potential bottlenecks are reduced and the calculated conductance increased to $G = 0.82g_0$ from its lower value ($G = 0.58g_0$) for the dimerized wire discussed in the text. Such sensitivity to small variations in the inter-electrode distance, as well as the variation of interatomic distances in the wire due to thermal effects, may account for significant variations in the measured conductance at the final stages of elongation and consequently may affect the correlation between the measured tip-to-tip distances and the recorded conductance (which is reported to be about $1g_0$ for a tip-to-tip distance of 8.9 Å, see Figure 3 in ref 6.